

RESEARCH

Open Access

Effect of gas blowing on the head of thermal ablation vehicle



Qing Li^{1,2}, Xianxu Yuan^{1,2*} , Jianqiang Chen^{1,2} and Lin Bi^{1,2}

*Correspondence:

yuanxianxu@cardc.cn

¹ State Key Laboratory of Aerodynamics, China Aerodynamics Research and Development Center, Mianyang 621000, China
Full list of author information is available at the end of the article

Abstract

The reentry vehicle will encounter thermal ablation, especially at the stagnation point regime. A theoretical work has been done to analyze the thermal effect of gas blowing due to thermal ablation of surface material on the head of a general hypersonic vehicle. By deriving the formulation, research takes into account the effect of gas blowing on the thermal dynamics balance, and then solves them by numerical discretization. It is found that gas blowing will increase the temperature and heat flux at the surface of stagnation point regime.

Keywords: Stagnation point flow, Viscous compression of fluid parcel, Gas blowing

1 Introduction

Reentry vehicle is crucial for many aerodynamic applications, such as Luna or Moon probe project, etc. One inevitable issue is that the stagnation point of the reentry body usually experiences very high temperature, leading to the thermal ablation problem [1–10]. The thermal ablation problem is a multi-physics process. In general, the detached bow shock wave forms over the head of hypersonic vehicle [11–13], the fluid flow is compressed and its thermal dynamic properties such as density, pressure and temperature increase significantly [14, 15]. The temperature of the air is ten thousand degrees, the air is dissociated electrically and chemical reactions happen simultaneously [16, 17]. Moreover, the solid material on the surface of the vehicle reacts with the ambient fluid flow due to very high temperature, the reaction products are the multi-component gas, and the no-slip and no-penetration wall condition for Navier-Stokes fluid dynamics model is no longer valid [1, 6–8]. This is one of the mass loss mechanisms of thermal ablation. Another mechanism is that, the solid particle erodes from the surface because the high temperature alters the mechanics properties of surface material, and then the ambient fluid flow carries out the surface mass in forms of rod particles [1]. The mass loss mechanism is important, because it changes the aerodynamic geometry of the vehicle; thus the aerodynamic force and heat flux is changed as well [1]. In addition, the solid particles go into the downstream boundary layer, which will affect the transition [18, 19] and turbulence [20, 21] over the surface of the vehicle, making the aerodynamic force and heat flux prediction become

complicated [22, 23] to predict. It is worth noting that, the solid material experiences a chemical reaction under high temperature of fluid flow at stagnation point regime [1, 6–8]. Therefore, thermal dynamics of single phase stagnation point flow is one of the crucial factors to understand the complicated mass loss process during the thermal ablation.

Research focuses our attention on the near wall of thermal dynamics of the stagnation point regime of a sphere with typical physical properties. According to the dimensionless analysis, the local Mach number in the near wall regime is approximately zero due to the local high sonic speed, so we assume that the stagnation point flow in the very near wall regime of our objective problem is incompressible. If taking incompressible stagnation point flow as a prototype model to study, there are differences. The multi-physics nature of thermal ablation makes the wall inject gas into the stagnation point regime, while the effect of gas blowing on the thermal dynamics is not clear.

Research studies this effect on the thermal dynamics of a compressible stagnation point flow in a typical hypersonic vehicle cruising condition by means of theoretical research, so as to have some qualitative understanding of the thermal ablation problem, paving the way for future study and planning.

2 Physical problem

2.1 Incompressible assumption in the near wall region

Firstly, in order not to lose generality, we consider a prototype of hypersonic incoming flow passing a sphere, with physical properties of air being that of altitude height around 20 ~ 30 km, which is typical parameter ranges where thermal ablation happens, see Fig. 1. By default, all the physical parameters in this paper use the ISO unit. In the current study, the typical incoming flow Mach number is around $M_1 = 8 \sim 20$, the density of fluid flow is $\rho_1 = 1.8 \times 10^2 \text{ kg/m}^3$, the temperature is $T_1 = 226.5 \text{ K}$, the pressure is $p_1 = 1197.0 \text{ Pa}$, the sound speed is $a_1 = 301.7 \text{ m/s}$, the fluid flow velocity is $U_1 = 6034.0 \text{ m/s}$, the dynamic viscosity is $\mu_1 = 1.5 \times 10^{-5} \text{ Pa} \cdot \text{s}$, and the kinematic viscosity is $\nu_1 = 8.2 \times 10^{-4} \text{ m}^2/\text{s}$. The incoming flow forms a detached shock wave over the sphere which can be seen in many hypersonic vehicles; behind the shock wave, the fluid flow is compressed, its entropy increases, its thermal dynamics properties, such as pressure, density and temperature increase significantly as well, and the chemical reaction of air happens due to high temperature [16, 17]. Having assumed the gas being in a perfect state, research focuses attention on the stagnation point flow region and considers neither the chemical reaction nor the electric dissociation. Therefore, research calculates the flow and thermal dynamics properties by normal shock relations [14, 15], see Eqs. (1)–(6). Let's take $M_1 = 20$ as an example, the properties behind the normal shock wave can be calculated, with the Mach number being $M_2 = 0.4$, the density of fluid flow being $\rho_2 = 0.1 \text{ kg/m}^3$, the temperature being $T_2 = 1.8 \times 10^4 \text{ K}$, the pressure being $p_2 = 5.5 \times 10^4 \text{ Pa}$, the sound speed being $a_2 = 2667.0 \text{ m/s}$, the fluid flow velocity being $U_2 = 1006.0 \text{ m/s}$, the dynamic viscosity being $\mu_2 = 1.9 \times 10^4 \text{ Pa} \cdot \text{s}$, and the kinematic viscosity being $\nu_2 = 1.8 \times 10^{-3} \text{ m}^2/\text{s}$. In addition, it is found that,

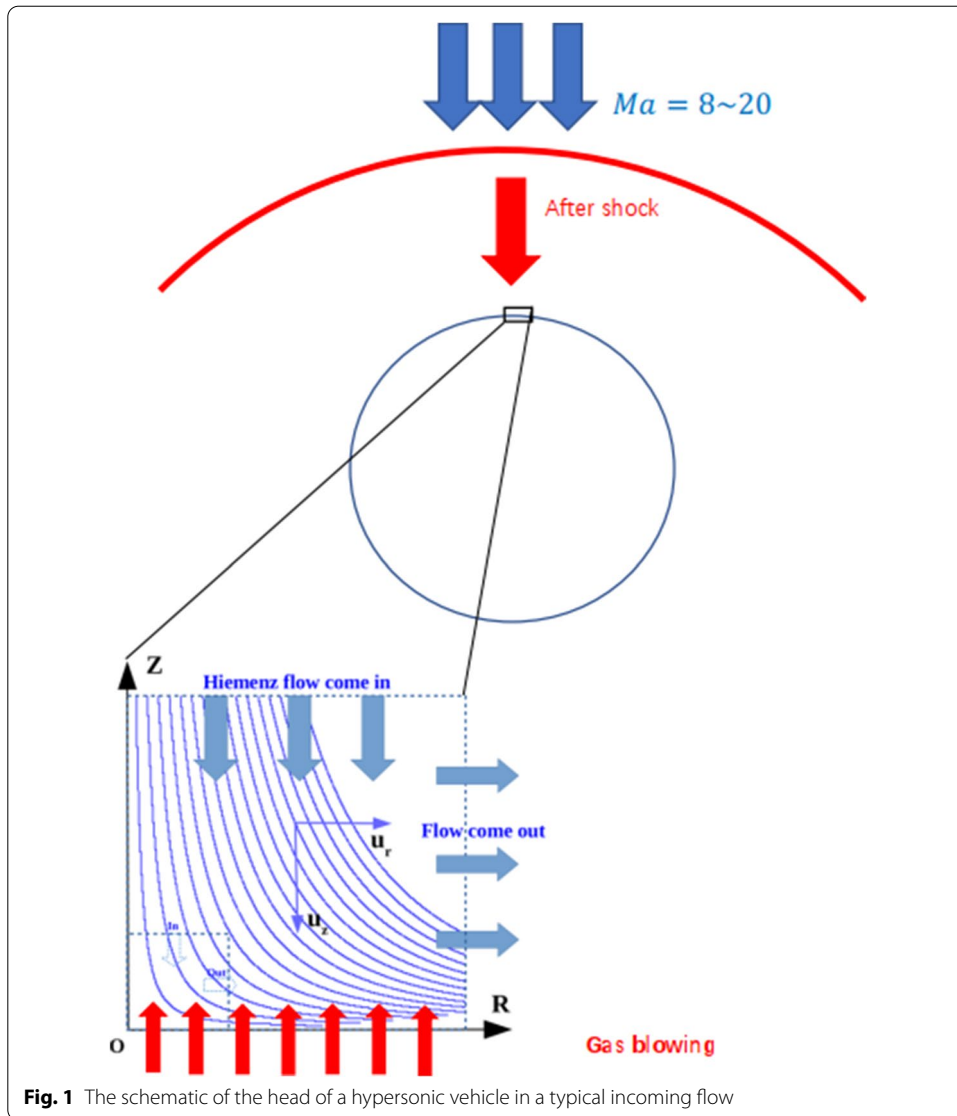


Fig. 1 The schematic of the head of a hypersonic vehicle in a typical incoming flow

for $M_1 = 8 \sim 20$, the physical properties behind the shock wave are in the same order, and the variations are small.

$$M_2 = \sqrt{\frac{1 + \frac{\gamma-1}{2}M_1^2}{\gamma M_1^2 - \frac{\gamma-1}{2}}} \tag{1}$$

$$\frac{U_2}{U_1} = \frac{\gamma-1}{\gamma+1} + \frac{2}{(\gamma+1)M_1^2} \tag{2}$$

$$\frac{p_2}{p_1} = -\frac{\gamma-1}{\gamma+1} + \frac{2\gamma}{(\gamma+1)}M_1^2 \tag{3}$$

$$\frac{\rho_2}{\rho_1} = \frac{\frac{\gamma+1}{2}M_1^2}{1 + \frac{\gamma-1}{2}M_1^2} \tag{4}$$

$$\frac{T_2}{T_1} = \left(\frac{a_2}{a_1}\right)^2 = \frac{2}{(\gamma+1)M_1^2} \left(\frac{2\gamma}{\gamma+1}M_1^2 - \frac{\gamma-1}{\gamma+1}\right) \left(1 + \frac{\gamma-1}{2}M_1^2\right) \tag{5}$$

$$a_1 = \sqrt{\gamma RT_1}, a_2 = \sqrt{\gamma RT_2} \tag{6}$$

Secondly, the detached distance of detached shock wave can be estimated by a semi-empirical relation [11–13], see Eq. (7), which is weakly related to chemical reactions [13, 24, 25]. D is the typical diameter of blunt nose hypersonic vehicle, with $D=0.2\text{m}$, δ_h being the distance of detached shock wave, and $\delta_h = 13.8e - 3\text{m}$ estimated by Eq. (7), see Fig. 1.

$$\frac{\delta_h}{D} = 0.41 \frac{\rho_1}{\rho_2} \tag{7}$$

Research considers the near wall fluid dynamics behind the shock wave as a stagnation point flow, see Fig. 1. Keep in mind that the fluid flow is a compressible flow, which increases the complexity of the problem. In light of this, research investigates the local Mach number of near wall fluid dynamics of stagnation point flow. The bulk compression rate of stagnation point flow can be estimated as [26–29] $B = U_2/\delta_h \simeq 3.6 \times 10^4\text{s}^{-1} \sim O(10^4\text{s}^{-1})$, with the bulk viscous boundary layer thickness of stagnation point flow being $\delta = \sqrt{\nu_2/B} \simeq 22.4 \times 10^{-5}\text{m}$, and the ratio between boundary layer thickness and detached distance being $\frac{\delta}{\delta_h} \sim \frac{1}{60}$.

Assume that the fluid flow velocity of the stagnation point flow behind the shock wave decreases linearly $\frac{U_\tau}{U_2} = \frac{\delta}{\delta_h}$ within the near wall region $Z = O(\delta)$, with the local fluid velocity being $U_\tau \simeq \frac{1}{60}U_2 \sim O(10\text{m/s})$, and the local sound speed being $a_2 = \sqrt{\gamma RT_2} \sim O(10^3\text{m/s})$. Ultimately, the local Mach number in the near wall region is estimated as $M_\tau \simeq \frac{U_\tau}{a_2} \sim O(0.01)$; thus in the near wall region, the fluid dynamics can be approximately treated as incompressible fluid flow, which gives much mathematical convenience in theoretical analysis in later sections.

2.2 Objective problem: effect of gas blowing on the thermal dynamics of stagnation point flow

Behind the detached shock wave, the fluid flow will have very high temperature $T_2 = 1.8 \times 10^4\text{K}$, the local Mach number is around $M_\tau \sim O(0.01)$, the chemical reaction and electric dissociation will happen as well. For simplification, research considers neither the chemical reaction nor the electric dissociation. The flow behind the shock wave locally forms a stagnation point flow at the head of hypersonic vehicle. Research focuses attention on the near wall of stagnation point flow, where the incompressible assumption will hold, $M_\tau \sim O(0.01)$. The current study aims to understand one question: what's the effect of gas blowing on it.

3 Effect of gas blowing on thermal dynamics at stagnation point region

3.1 Traditional incompressible dynamic and thermal dynamic equations

In the following, theoretical analysis is conducted in the Cartesian coordinate system, where coordinate (x, y) represents (R, Z) , and velocity $[u, v]^T$ represents $[u_r, u_z]^T$ in Fig. 1, respectively.

$$\begin{aligned} \nabla \cdot U &= 0, U = [u, v]^T \\ \rho U \cdot \nabla U &= -\nabla p + \mu \Delta U \end{aligned} \tag{8}$$

$$\rho C_p (U \cdot \nabla T) = k \Delta T \tag{9}$$

$$\frac{u}{U_\infty} = \frac{x}{\delta_\infty} f'(\eta), \frac{v}{U_\infty} = -f(\eta) \tag{10}$$

$$\eta = \frac{y}{\delta_\infty}, \delta_\infty = \sqrt{\frac{v}{B}}, U_\infty = \sqrt{Bv} \tag{11}$$

$$\theta(\eta) = \frac{T(\eta) - T_w}{T_\infty - T_w}, Pr = \frac{C_p \mu}{k} \tag{12}$$

$$f''' + ff'' + 1 - f'^2 = 0 \tag{13}$$

$$\theta'' + Pr f \theta' = 0 \tag{14}$$

Keep in mind that the local Mach number is around zero $M_r \sim 0$, allowing us to use incompressible Hiemenz flow to analyze the thermal dynamics of objective problem.

In order to keep generality, research takes full 2D N-S equations to begin, see Eqs. (8)–(9).

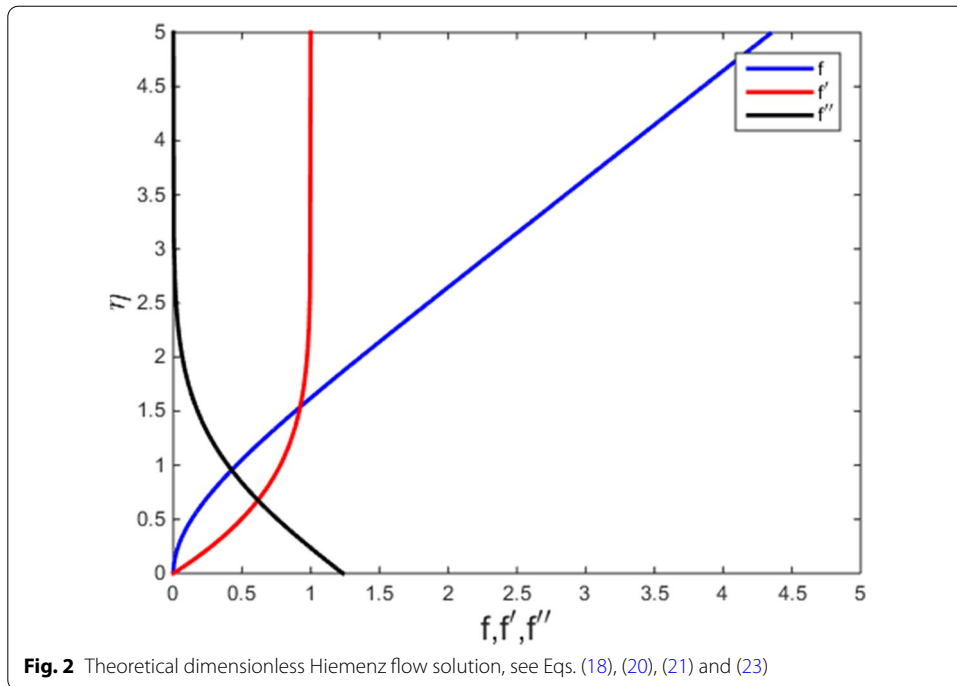
In order to better understand the problem, research firstly examines the standard Hiemenz solution without thermal dynamics equation.

Take $f(0)=0, f'(0)=0, f''(0)=1.2326$ to integrate numerically by the Runge-Kutta 4th order method, the Ordinary Equation System [30], and then theoretical solution can be found as Fig. 2 indicates. Keep in mind that the wall normal velocity $v(y)$ is proportional to $\sim f(\eta)$, the streamwise velocity $u(x, y)$ is proportional to $\sim x \cdot f'(\eta)$, and the viscous dissipation $\frac{\partial u(x, y)}{\partial y}$ is proportional to $\sim f''(\eta)$. Inside the viscous boundary layer $\eta < \frac{y}{\delta_\infty} = 3$, the dimensionless viscous dissipation $f''(\eta)$ is not zero, but the maximum at wall; outside the viscous boundary layer, $\eta = \frac{y}{\delta_\infty} = 3$, the dimensionless viscous dissipation $f''(\eta)$ vanishes, and dimensionless velocities f and f' become linear strain flow velocities.

3.2 Theoretical derivation of effect of gas blowing and suction on thermal dynamics

For the case of blowing gas from bottom wall at stagnation point regime, the governing equations are Eqs. (15)–(18):

$$f_w = -5 < 0 \text{ (blowing)}, \eta = 0 \tag{15}$$



$$f(\eta) = f_w(1 - \varphi(z)), z = -\frac{\eta}{f_w} \tag{16}$$

$$(\varphi - 1)\varphi'' - \varphi'^2 = 0, \varphi(\eta) = \eta - 1 + e^{-\eta} \tag{17}$$

$$\theta'' + Prf\theta' = 0 \tag{18}$$

Similarly, for the case of suction gas from bottom wall at stagnation point regime, the governing equations are Eqs. (19)-(22):

$$f_w = 5 > 0 \text{ (suction)}, \eta = 0 \tag{19}$$

$$f(\eta) = f_w + \frac{1}{f_w}\varphi(z), z = f_w\eta \tag{20}$$

$$\varphi''' + \varphi'' = 0, \varphi(\eta) = 1 - \cos(z) \tag{21}$$

$$\theta'' + Prf\theta' = 0 \tag{22}$$

In this section, thermal dynamics balance is controlled by heat conduction and fluid convection. The gas blowing effect will alter the dynamics of stagnation point flow, so as to indirectly influence the thermal dynamics by convection effect. Eqs. (15)-(18)

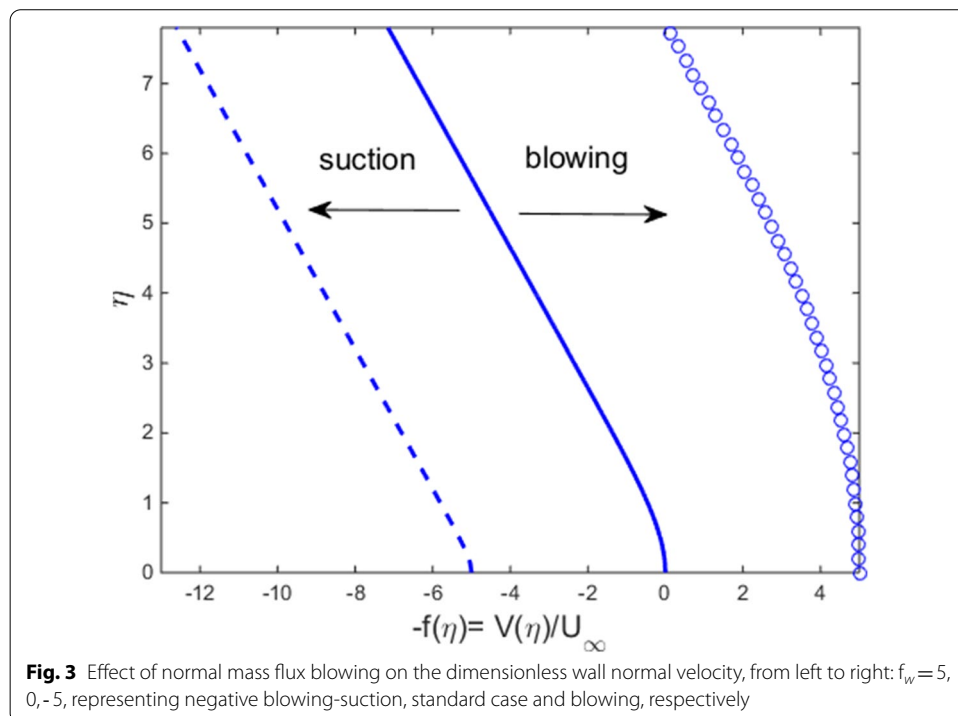
represent the dynamics with gas blowing [31], while Eqs. (19)–(22) represent the dynamics with gas suction [31].

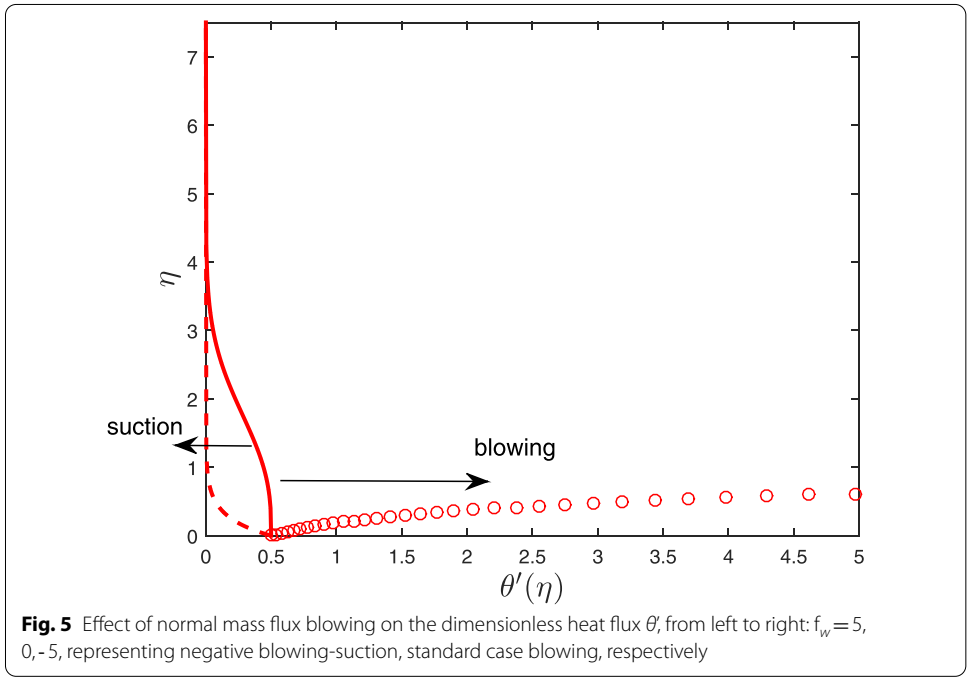
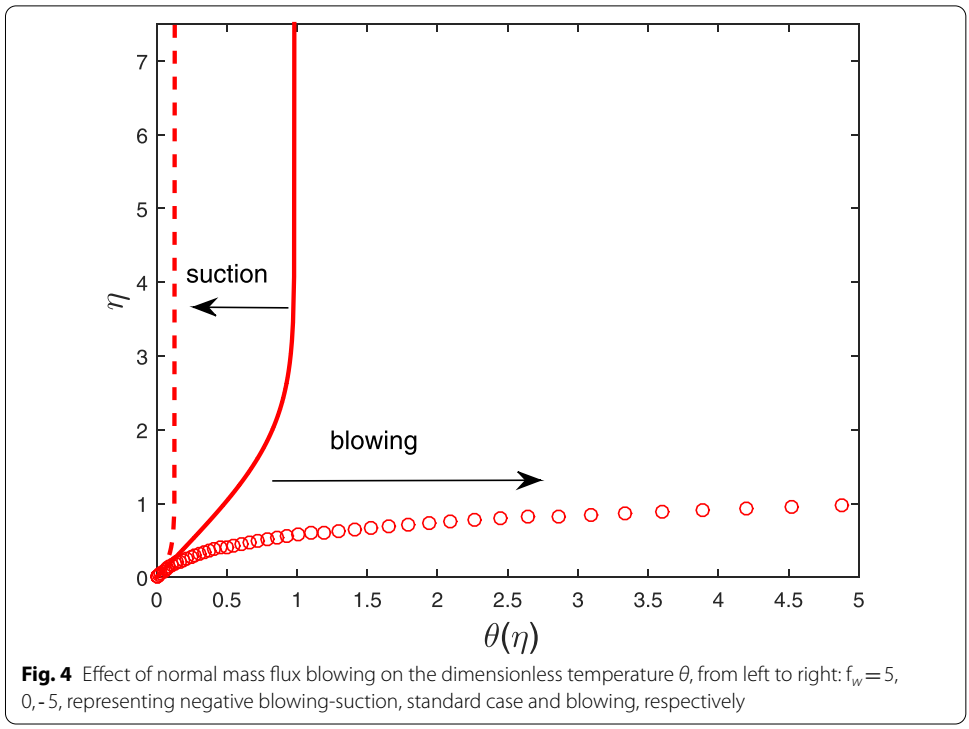
Set $f(0) = 0, f'(0) = 0, f''(0) = 1.2326$ to satisfy the no-slip and no-penetration wall boundary condition for standard, blowing and suction cases, the gas injection effect can be represented by dimensionless mass flux f_w . Set $\theta(0) = 0, \theta'(0) = 0.0$ for thermal dynamics boundary condition at wall. Then integrate numerically by the Runge-Kutta 4th order method, the ODE system Eq. (17) and Eq. (18) for blowing case; integrate the ODE system Eq. (21) and Eq. (22) for suction case.

3.3 Results and discussions

Figure 3 shows that, the effect of dimensionless mass flux f_w on the wall normal velocity is to increase or decrease the wall normal velocity. Keep in mind that, thermal dynamics balance is controlled by heat conduction $k \frac{\partial^2 T}{\partial y^2}$ and fluid flow convection $\rho C_p v \frac{\partial T}{\partial y}$, and the variation of wall normal velocity profile $v(\eta)$ will surely alter the thermal dynamics balance.

Figures 4 and 5 show the effect of dimensionless mass flux f_w on the dimensionless temperature θ and dimensionless heat flux θ' of stagnation point flow. It is clear that, the blowing increases significantly the temperature and heat flux, while suction does the contrast. This means that: in reality, thermal ablation-induced gas injection will deteriorate the heat environment of hypersonic vehicle. In terms of the effect of suction, the current conclusion is purely academic. In reality, if the very hot fluid flow is sucked into the vehicle body, the heat will be accumulated, which means it is impossible to use suction to actively control the heat over the vehicle surface, although the current study suggests that suction will diminish the surface temperature and heat flux. Nevertheless,





it is valuable for basic research, which provides many options and basic knowledge for the final design.

4 Conclusion

Research conducted theoretical analysis on the thermal dynamics of stagnation point flow regime of a general hypersonic vehicle. The effect of gas blowing due to thermal ablation on the thermal dynamics has been studied by theoretical derivation of new ODE.

In terms of effect of gas blowing, increment of mass flux of gas blowing will deteriorate the heat environment of stagnation point flow, because the normal fluid convective effect on the heat is augmented by the wall normal mass flux. However, the current conclusion is based on the assumption: the gas injection temperature is by default equal to the wall temperature, and when it comes to the application, practical caution is needed. Similarly, the suction will alleviate the heat flux, but in practice, when such extreme high temperature gas is sucked into the vehicle head, the thermal ablation resist material reacts, and the material mechanical properties are deteriorated. Therefore, the current research results serve as a qualitative direction for basic understanding of thermal dynamics of hypersonic stagnation point flow.

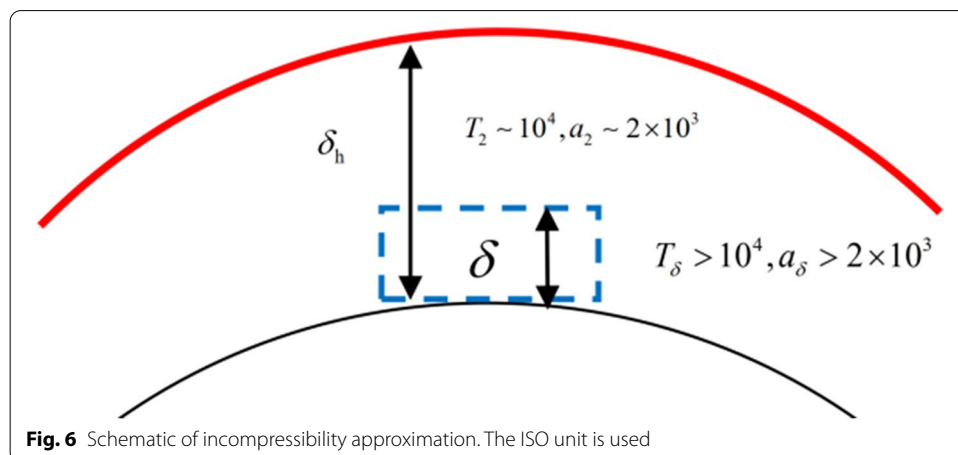
Appendix

Explanation of incompressible approximation

Figure 6 represents the dimensional analysis on a hypersonic stagnation point flow. The typical particle diameter is around $d_p \sim 10^{-5}$ m, and the computational domain character length is around $\sim 10d_p \sim 10^{-4}$ m $\sim \delta$.

The detached shock wave distance from the wall δ_h , and its relation with δ in terms of order are: $\delta_h \approx 120 \times 10^{-4}$ m, $\delta \approx 2 \times 10^{-4}$ m, $\delta_h/\delta = 60$.

According to the theoretical solution of Hiemenz flow, far from the bottom wall, larger than δ , fluid parcel vertical velocity can be approximately estimated as inviscid strain



flow $V = -By$. The value of interest domain velocity is V_δ at δ , and that of velocity behind the detached shock is $V_{\delta_h} \approx 1000$ m/s at δ_h .

The linear relation of the theoretical solution of Hiemenz flow can be used to estimate the order of velocity in the computational domain:

$$\frac{V_\delta}{\delta} \approx \frac{V_{\delta_h}}{\delta_h}, V_\delta \approx \frac{\delta}{\delta_h} V_{\delta_h} = \frac{1}{60} 1000 \approx 16 \text{ m/s}$$

In the stagnation point regime, the temperature can be estimated: $T_\delta > 10^4$ K, $a_\delta > 2 \times 10^3$ m/s, $V_\delta \approx 16$ m/s and the local sonic speed is around $a_\delta \approx 2000$ m/s, thus $M_\delta = \frac{V_\delta}{a_\delta}$.

According to the definition,

$$M_\delta = \frac{16 \text{ m/s}}{a_\delta > 2000 \text{ m/s}} \approx 0.01,$$

in this respect, the blue interest domain can be treated as incompressible. In detail, starting from complete compressible fluid dynamic equations, and introducing with prior knowledge $M_\delta \approx 0.01$, the incompressible approximation can be proved.

Firstly, some important dimensional and dimensionless parameters will be defined as follows:

$$\begin{aligned} Re &= \frac{\rho_\infty U_\infty L_\infty}{\mu_\infty}, Pr = \frac{C_p \mu_\infty}{k_\infty}, Ma = \frac{U_\infty}{a_\infty}, \\ a_\infty &= \sqrt{\gamma R T_\infty}, p_\infty = \rho_\infty U_\infty^2 \\ C_v &= \frac{R}{\gamma - 1}, C_v^* = \frac{1}{\gamma(\gamma - 1) Ma^2}, Str = \frac{L_\infty}{U_\infty t_\infty} = 1, \\ \phi &= \nabla \cdot \left(\vec{u} \cdot \mu \nabla \vec{u} + \vec{u} \cdot \mu \nabla \vec{u}^T - \vec{u} \cdot \bar{I} \frac{2\mu}{3} \nabla \cdot \vec{u} \right) \\ f &= f^* f_\infty \left(ex : \nabla = \frac{\nabla^*}{L_\infty}, \partial t^* \cdot t_\infty = \partial t, \vec{u}^* U_\infty = \vec{u} \dots etc \right) \end{aligned}$$

∞ represents the reference physical variable, and it can be the value at infinite far field, or certain specific regime that we are interested in. For example, for wall-bounded turbulence, the reference velocity is $U_\infty = U_r$, while for homogeneous turbulence, it is $U_\infty = U_\lambda$.

$$\begin{aligned} \text{Reference mass flux: } \frac{\rho_\infty U_\infty}{L_\infty} &= \left(\frac{\rho_\infty U_\infty}{L_\infty^3} \right) L_\infty^2 \\ \text{Reference momentum flux: } \frac{\rho_\infty U_\infty^2}{L_\infty} &= \left(\frac{\rho_\infty U_\infty^2}{L_\infty^3} \right) L_\infty^2 \\ \text{Reference energy flux: } \frac{\rho_\infty U_\infty^3}{L_\infty} &= \left(\frac{\rho_\infty U_\infty^3}{L_\infty^3} \right) L_\infty^2 \end{aligned}$$

Three basic control equations:

mass conservation:

$$\frac{L_\infty}{\rho_\infty U_\infty} \left(\frac{\partial \rho}{\partial t} + \nabla \cdot \vec{u} = 0 \right) \tag{23}$$

momentum conservation:

$$\frac{L_\infty}{\rho_\infty U_\infty^2} \left\{ \frac{\partial \rho \vec{u}}{\partial t} + \nabla \cdot \left(\rho \vec{u} \otimes \vec{u} + \bar{I} p \right) \right\} = \frac{L_\infty}{\rho_\infty U_\infty^2} \left\{ \nabla \cdot \left(\mu \nabla \vec{u} + \mu \nabla \vec{u}^T - \bar{I} \frac{2\mu}{3} \nabla \cdot \vec{u} \right) \right\} \tag{24}$$

energy conservation:

$$\begin{aligned} & \frac{L_\infty}{\rho_\infty U_\infty^3} \left\{ \frac{\partial \rho C_V T}{\partial t} + \frac{\partial \rho \frac{|V|^2}{2}}{\partial t} + \nabla \cdot (\rho C_V T \vec{u}) + \nabla \cdot \left(\rho \vec{u} \frac{|V|^2}{2} \right) + \nabla \cdot \left(\bar{I} \cdot \vec{u} p \right) \right\} \\ = & \frac{L_\infty}{\rho_\infty U_\infty^3} \left\{ -\nabla \cdot (-k \nabla T) + \nabla \cdot \left(\vec{u} \cdot \mu \nabla \vec{u} + \vec{u} \cdot \mu \nabla \vec{u}^T - \vec{u} \cdot \bar{I} \frac{2\mu}{3} \nabla \cdot \vec{u} \right) \right\} \end{aligned} \tag{25}$$

dimensionless mass conservation:

$$Str \cdot \frac{\partial \rho^*}{\partial t^*} + \nabla^* \cdot \vec{u}^* = 0 \tag{26}$$

dimensionless momentum conservation:

$$\begin{aligned} & Str \cdot \frac{\partial \rho^* \vec{u}^*}{\partial t^*} + \nabla^* \cdot \left(\rho^* \vec{u}^* \otimes \vec{u}^* + \bar{I} p^* \right) \\ = & \frac{1}{Re} \nabla^* \cdot \left(\mu^* \nabla^* \vec{u}^* + \mu^* \nabla^* \vec{u}^{*T} - \bar{I} \frac{2\mu^*}{3} \nabla^* \cdot \vec{u}^* \right) \end{aligned} \tag{27}$$

dimensionless energy conservation:

$$\begin{aligned} & \frac{L_\infty}{\rho_\infty U_\infty^3} \left\{ \frac{\rho_\infty \frac{R}{\gamma-1} T_\infty}{t_\infty} \frac{\partial \rho^* T^*}{\partial t^*} + \frac{\rho_\infty U_\infty^2}{t_\infty} \frac{\partial \rho^* \frac{|V^*|^2}{2}}{\partial t^*} + \frac{\rho_\infty \frac{R}{\gamma-1} T_\infty U_\infty}{L_\infty} \nabla^* \cdot \left(\rho^* T^* \vec{u}^* \right) + \right. \\ & \left. \frac{\rho_\infty U_\infty^3}{L_\infty} \nabla^* \cdot \left(\rho^* \vec{u}^* \frac{|V^*|^2}{2} \right) + \frac{\rho_\infty U_\infty^3}{L_\infty} \nabla^* \cdot \left(\bar{I} \cdot \vec{u}^* p^* \right) \right\} \\ = & \frac{L_\infty}{\rho_\infty U_\infty^3} \left\{ \frac{k_\infty T_\infty}{L_\infty^2} \nabla^* \cdot (k^* \nabla^* T^*) + \frac{\mu_\infty U_\infty^2}{L_\infty^2} \phi^* \right\} \end{aligned} \tag{28}$$

Due to the complexity of energy equation, the terms are developed one by one in details as follows:

1st term: unsteadiness of internal and pressure energy of fluid parcel

$$\begin{aligned} & \frac{L_\infty}{\rho_\infty U_\infty^3} \frac{\rho_\infty \frac{R}{\gamma-1} T_\infty}{t_\infty} \frac{\partial \rho^* T^*}{\partial t^*} = \frac{L_\infty}{U_\infty t_\infty} \frac{RT_\infty}{U_\infty^2 (\gamma-1)} \frac{\partial \rho^* T^*}{\partial t^*} \\ = & Str \cdot \frac{1}{Ma^2 \gamma (\gamma-1)} \frac{\partial \rho^* T^*}{\partial t^*} = \frac{\partial \rho^* C_V^* T^*}{\partial t^*} \end{aligned}$$

2nd term: unsteadiness of kinetic energy of fluid parcel

$$\frac{L_\infty}{\rho_\infty U_\infty^3} \frac{\rho_\infty U_\infty^2}{t_\infty} \frac{\partial \rho^* \frac{|V^*|^2}{2}}{\partial t^*} = Str \cdot \frac{\partial \rho^* \frac{|V^*|^2}{2}}{\partial t^*} = \frac{\partial \rho^* \frac{|V^*|^2}{2}}{\partial t^*}$$

3rd term: convection of internal and pressure energy of fluid parcel

$$\frac{L_\infty}{\rho_\infty U_\infty^3} \frac{\rho_\infty \frac{R}{\gamma-1} T_\infty U_\infty}{L_\infty} \nabla^* \cdot \left(\rho^* T^* \vec{u}^* \right) = \nabla^* \cdot \left(\rho^* C_V^* T^* \vec{u}^* \right)$$

4th term: convection of kinematic energy of fluid parcel

$$\frac{L_\infty}{\rho_\infty U_\infty^3} \frac{\rho_\infty U_\infty^3}{L_\infty} \nabla^* \cdot \left(\rho^* \vec{u}^* \frac{|V^*|^2}{2} \right) = \nabla^* \cdot \left(\rho^* \vec{u}^* \frac{|V^*|^2}{2} \right)$$

5th term: pressure gradient work $\vec{u}^* \cdot \nabla^* p^*$ and pressure work on the compressible fluid parcel $p^* \nabla^* \cdot \vec{u}^*$

$$\frac{L_\infty}{\rho_\infty U_\infty^3} \frac{\rho_\infty U_\infty^3}{L_\infty} \nabla^* \cdot (\bar{I} \cdot \vec{u}^* p^*) = \nabla^* \cdot (\bar{I} \cdot \vec{u}^* p^*)$$

6th term: heat conduction

$$\begin{aligned} \frac{L_\infty}{\rho_\infty U_\infty^3} \frac{k_\infty T_\infty}{L_\infty^2} \nabla^* \cdot (k^* \nabla^* T^*) &= \frac{1}{\rho_\infty U_\infty L_\infty} \frac{\mu}{\mu} \frac{C_v}{C_v} \frac{k_\infty T_\infty}{U_\infty^2} \nabla^* \cdot (k^* \nabla^* T^*) \\ &= \frac{1}{Re} \frac{1}{Pr} \frac{C_v T_\infty}{U_\infty^2} \nabla^* \cdot (k^* \nabla^* T^*) = \frac{1}{Re} \frac{1}{Pr} \frac{\gamma R T_\infty}{\gamma(\gamma-1)U_\infty^2} \nabla^* \cdot (k^* \nabla^* T^*) \\ &= \frac{1}{Re} \frac{1}{Pr} \frac{1}{(\gamma-1)Ma^2} \nabla^* \cdot (k^* \nabla^* T^*) \end{aligned}$$

7th term: viscous work on the fluid parcel

$$\frac{L_\infty}{\rho_\infty U_\infty^3} \frac{\mu_\infty U_\infty^2}{L_\infty^2} \nabla^* \cdot (\vec{u}^* \cdot \mu^* \nabla^* \vec{u}^*) = \frac{1}{Re} \phi^*$$

dimensionless energy conservation:

$$\begin{aligned} \frac{\partial \rho^* C_v^* T^*}{\partial t^*} + \frac{\partial \rho^* \frac{|V^*|^2}{2}}{\partial t^*} + \nabla^* \cdot (\rho^* C_v^* T^* \vec{u}^*) + \\ \nabla^* \cdot \left(\rho^* \vec{u}^* \frac{|V^*|^2}{2} \right) + \nabla^* \cdot (\bar{I} \cdot \vec{u}^* p^*) \\ = \frac{1}{Re} \frac{\gamma}{Pr} C_v^* \nabla^* \cdot (k^* \nabla^* T^*) + \frac{1}{Re} \phi^* \end{aligned} \tag{29}$$

dimensionless energy conservation $\cdot \gamma(\gamma-1)Ma^2$:

$$\begin{aligned} \gamma(\gamma-1)Ma^2 \left\{ \frac{\partial \rho^* C_v^* T^*}{\partial t^*} + \frac{\partial \rho^* \frac{|V^*|^2}{2}}{\partial t^*} + \nabla^* \cdot (\rho^* C_v^* T^* \vec{u}^*) + \right. \\ \left. \nabla^* \cdot \left(\rho^* \vec{u}^* \frac{|V^*|^2}{2} \right) + \nabla^* \cdot (\bar{I} \cdot \vec{u}^* p^*) \right\} \\ = \gamma(\gamma-1)Ma^2 \left\{ \frac{1}{Re} \frac{\gamma}{Pr} C_v^* \nabla^* \cdot (k^* \nabla^* T^*) + \frac{1}{Re} \phi^* \right\} \end{aligned} \tag{30}$$

$$\begin{aligned} \frac{\partial \rho^* T^*}{\partial t^*} + \gamma(\gamma-1)Ma^2 \frac{\partial \rho^* \frac{|V^*|^2}{2}}{\partial t^*} + \nabla^* \cdot (\rho^* T^* \vec{u}^*) + \\ \gamma(\gamma-1)Ma^2 \nabla^* \cdot \left(\rho^* \vec{u}^* \frac{|V^*|^2}{2} \right) + \gamma(\gamma-1)Ma^2 \nabla^* \cdot (\bar{I} \cdot \vec{u}^* p^*) \\ = \frac{1}{Re} \frac{\gamma}{Pr} \nabla^* \cdot (k^* \nabla^* T^*) + \gamma(\gamma-1)Ma^2 \frac{1}{Re} \phi^* \end{aligned}$$

Thus, it is clear that, when $\gamma(\gamma-1)Ma^2$ becomes vanishingly small, certain terms can be neglected, which are the kinetic energy of fluid parcel, the pressure gradient and pressure work on the fluid parcel, and the viscous work on the fluid parcel.

$$\begin{aligned} \frac{\partial \rho^* T^*}{\partial t^*} + \gamma(\gamma-1)Ma^2 \frac{\partial \rho^* \frac{|V^*|^2}{2}}{\partial t^*} + \nabla^* \cdot (\rho^* T^* \vec{u}^*) + \gamma(\gamma-1)Ma^2 \nabla^* \cdot \left(\rho^* \vec{u}^* \frac{|V^*|^2}{2} \right), \\ \gamma(\gamma-1)Ma^2 \nabla^* \cdot (\bar{I} \cdot \vec{u}^* p^*), \\ \gamma(\gamma-1)Ma^2 \frac{1}{Re} \phi^* \end{aligned}$$

Once $M_\tau = M_\delta \approx 0.01$, the energy equation can be simplified as:

$$\frac{\partial \rho^* T^*}{\partial t^*} + \nabla^* \cdot (\rho^* T^* \vec{u}^*) = \frac{1}{Re Pr} \nabla^* \cdot (k^* \nabla^* T^*) \tag{31}$$

dimensionless mass conservation:

$$\frac{\partial \rho^*}{\partial t^*} + \nabla^* \cdot \vec{u}^* = 0 \tag{32}$$

dimensionless momentum conservation:

$$\begin{aligned} \frac{\partial \rho^* \vec{u}^*}{\partial t^*} + \nabla^* \cdot (\rho^* \vec{u}^* \otimes \vec{u}^* + \bar{I} p^*) = \\ \frac{1}{Re} \nabla^* \cdot \left(\mu^* \nabla^* \vec{u}^* + \mu^* \nabla^* \vec{u}^{*T} - \bar{I} \frac{2\mu^*}{3} \nabla \cdot \vec{u}^* \right) \end{aligned} \tag{33}$$

dimensionless energy conservation:

$$\frac{\partial \rho^* T^*}{\partial t^*} + \nabla^* \cdot (\rho^* T^* \vec{u}^*) = \frac{1}{Re Pr} \nabla^* \cdot (k^* \nabla^* T^*) \tag{34}$$

$\frac{\partial \rho}{\rho} = Ma^2 \frac{\partial u}{u} = 0, \partial \rho = 0, \rho = cte, \rho^* = cte = \frac{\rho}{\rho_\infty} = 1$, here ∞ represents the character physical variable in the near wall stagnation point regime, where $M_\delta \approx 0.01$.

dimensionless mass conservation:

$$0 + \nabla^* \cdot \vec{u}^* = 0 \tag{35}$$

dimensionless momentum conservation:

$$\begin{aligned} \frac{\partial \vec{u}^*}{\partial t^*} + \nabla^* \cdot (\vec{u}^* \otimes \vec{u}^* + \bar{I} p^*) = \\ \frac{1}{Re} \nabla^* \cdot \left(\frac{\mu^*}{\rho^*} \nabla^* \vec{u}^* + \frac{\mu^*}{\rho^*} \nabla^* \vec{u}^{*T} - \bar{I} \frac{2\mu^*}{3} \nabla \cdot \vec{u}^* \right) \end{aligned} \tag{36}$$

dimensionless energy conservation:

$$\frac{\partial T^*}{\partial t^*} + \nabla^* \cdot (T^* \vec{u}^*) = \frac{1}{Re Pr} \nabla^* \cdot \left(\frac{k^*}{\rho^*} \nabla^* T^* \right) \tag{37}$$

Therefore, the energy equation becomes the heat convection and conduction equation, and its influence on the dynamic equation alters the dynamic viscosity $\frac{\mu^*}{\rho^*}$, which is equivalent to the density stratification effect in incompressible fluid. Temperature-induced density stratification effect is beyond the scope of current study. In general, in near wall stagnation point regime with extreme high temperature, $M_\delta \sim 0$, the complete compressible fluid dynamic equations are retrograded into incompressible equations.

Acknowledgements

The authors would like to thank the National Key Research and Development Plan of China for providing the funding through the project No.2019YFA0405200.

Authors' contributions

The contribution of the authors to the work is equivalent. All authors read and approved the final manuscript.

Funding

This work was supported by the National Key Research and Development Plan of China through the project No.2019YFA0405200.

Availability of data and materials

The datasets used or analyzed during the current study are available from the corresponding author on reasonable request.

Declarations

Competing interests

The authors declare that they have no competing interests.

Author details

¹State Key Laboratory of Aerodynamics, China Aerodynamics Research and Development Center, Mianyang 621000, China. ²Computational Aerodynamics Institute, China Aerodynamics Research and Development Center, Mianyang 621000, China.

Received: 1 July 2021 Accepted: 18 November 2021

Published online: 09 March 2022

References

1. Guo Y, Shi W, Zeng L, Du B (2019) Mechanism of ablative thermal protection applied to hypersonic vehicles. Science Press, Beijing (in Chinese)
2. AFCRL (1974) AFCRL fiscal year 1975, Air Force technical objectives document. AFCRL-TR-74-0581
3. Huang Z (1981) Transient shape and inner temperature distribution of ablative cone head. *Acta Aerodyn Sin* 1:53–65 (in Chinese)
4. Zhang Z, Pan M, Liu C (2003) Hypersonic aerodynamic heat and thermal protection. National Defense Industry Press, Beijing (in Chinese)
5. Guo Y, Gui Y, Tong F, Dai G (2013) Research on ablating mechanism of C/ZrC composite materials. *Acta Aerodyn Sin* 31(1):22–26 (in Chinese)
6. Han J, Zhang J, Du S (1996) Oxidation behaviour of 3D fine weave pierced carbon-carbon composites at ultra-high temperatures. *Acta Aeronaut Astronaut Sin* 17(5):577–581 (in Chinese)
7. Yi F (2001) Ultra high temperature properties and ablative behaviors of carbonous thermal protective composites. Dissertation, Harbin Institute of Technology (in Chinese)
8. Zhang YL, Li HJ, Yao XY et al (2011) Oxidation protection of C/SiC coated carbon/carbon composites with Si-Mo coating at high temperature. *Corros Sci* 53(6):2075–2079
9. Reda DC (1979) Comparative transition performance of several nosetip materials as defined by ballistics-range testing. Paper presented at the 25th international instrumentation symposium, Anaheim, CA, 7 May 1979
10. Kowbel W, Chellappa V, Withers JC et al (1996) Applications of net-shape molded carbon-carbon composites in IC engines. *J Adv Mater* 27(4):2–7
11. Lobb RK (1964) Experimental measurement of shock detachment distance on spheres fired in air at hypervelocities. In: Nelson WC (ed) *The high temperature aspects of hypersonic flow*. AGARDograph, vol 68. Pergamon Press Ltd., Oxford, pp 519–527
12. Sinclair J, Cui X (2017) A theoretical approximation of the shock standoff distance for supersonic flows around a circular cylinder. *Phys Fluids* 29:026102
13. Olivier H (2000) A theoretical model for the shock stand-off distance in frozen and equilibrium flows. *J Fluid Mech* 413:345–353
14. Wu W (1983) *Fluid mechanics*. Peking University Press, Beijing (in Chinese)
15. Anderson JD Jr (1995) *Computational fluid dynamics: the basics with applications*. McGraw-Hill, Singapore
16. Luo K, Wang Q, Li Y, Li J, Zhao W (2021) Research progress on magnetohydrodynamic flow control under test conditions with high temperature real gas effect. *Chin J Theor Appl Mech* 53(6):1515–1531 (in Chinese)
17. Liu P, Li Q, Huang Z et al (2019) Interpretation of wake instability at slip line in rotating detonation. *Int J Comput Fluid Dyn* 32(8–9):379–394
18. Loisel V, Abbas M, Masbernat O et al (2015) Inertia-driven particle migration and mixing in a wall-bounded laminar suspension flow. *Phys Fluids* 27(12):123304
19. Lashgari I, Picano F, Brandt L (2015) Transition and self-sustained turbulence in dilute suspensions of finite-size particles. *Theor Appl Mech Lett* 5(3):121–125
20. Zhou T, Zhao L, Huang W et al (2020) Non-monotonic effect of mass loading on turbulence modulations in particle-laden channel flow. *Phys Fluids* 32(4):043304
21. Picano F, Breugem WP, Brandt L (2015) Turbulent channel flow of dense suspensions of neutrally buoyant spheres. *J Fluid Mech* 764:463–487
22. Renard N, Deck S (2016) A theoretical decomposition of mean skin friction generation into physical phenomena across the boundary layer. *J Fluid Mech* 790:339–367
23. Li W, Fan Y, Modesti D et al (2019) Decomposition of the mean skin-friction drag in compressible turbulent channel flows. *J Fluid Mech* 875:101–123
24. Hornung HG (1972) Non-equilibrium dissociating nitrogen flow over spheres and circular cylinders. *J Fluid Mech* 53:149–176
25. Wen CY, Hornung HG (1995) Non-equilibrium dissociating flow over spheres. *J Fluid Mech* 299:389–405
26. Vigolo D, Griffiths IM, Radl S et al (2013) An experimental and theoretical investigation of particle-wall impacts in a T-junction. *J Fluid Mech* 727:236–255

27. Li Q, Abbas M, Morris JF et al (2020) Near-wall dynamics of a neutrally buoyant spherical particle in an axisymmetric stagnation point flow. *J Fluid Mech* 892:A32
28. Li Q, Abbas M, Morris JF (2020) Particle approach to a stagnation point at a wall: viscous damping and collision dynamics. *Phys Rev Fluids* 5:104301
29. Li Q (2019) Near-wall dynamics of neutrally buoyant particles in a wall-normal flow: from viscous damping to collision. Dissertation, Institut National Polytechnique de Toulouse, France
30. White FM (2006) *Viscous fluid flow*, 3rd edn. McGraw-Hill. New York
31. Schlichting H (1979) *Boundary-layer theory*, 7th edn. McGraw-Hill. New York

Publisher's Note

Springer Nature remains neutral with regard to jurisdictional claims in published maps and institutional affiliations.

Submit your manuscript to a SpringerOpen[®] journal and benefit from:

- ▶ Convenient online submission
- ▶ Rigorous peer review
- ▶ Open access: articles freely available online
- ▶ High visibility within the field
- ▶ Retaining the copyright to your article

Submit your next manuscript at ▶ [springeropen.com](https://www.springeropen.com)
